



# Unwrapping Core–Shell Nanowires into Nanoribbon-Based Superstructures\*\*

Alexander Pevzner, Guy Davidi, Hagit Peretz-Soroka, Ehud Havivi, Zahava Barkay, Ronit Popovitz-Biro, Artium Khatchtourints, and Fernando Patolsky\*

The tremendous motivation to manipulate matter on the nanometer scale arises from the intriguing emergence of novel physical properties and the ability to engineer a material's attributes by controlled sculpting at the nanoscale. One-dimensional (1D) nanostructures,<sup>[1]</sup> nanowires (NWs) and nanotubes (NTs), the most common members of this family, have attracted extraordinary attention in recent years due to their remarkable properties, and have led to a broad range of applications.<sup>[1b,2]</sup> Nanoribbons (NRs), another common form of 1D nanostructures, exhibit thicknesses ranging from a fraction of a nanometer up to 100 nm, and lateral dimensions at least one order of magnitude greater than their thickness. Their remarkably small thickness may lead to flexural rigidities several orders of magnitude lower than that exhibited by their bulk counterparts,<sup>[3]</sup> thus qualitatively changing the nature of the parent material and allowing otherwise impossible, nonplanar geometry arrangements, in which NRs conform and bond to nearly any foreign surface. By virtue of these properties, 1D NRs, and 2D nanomembranes (NMs) display unusual electronic, electromechanical, thermoelectric, optoelectronic, optomechanical, and photonic properties of great technological value.<sup>[3b]</sup>

Current synthetic methods for the preparation of semiconducting NRs and NMs include: 1) thermal evaporation of II–IV semiconductor materials, for example ZnS; 2) the chemical or mechanical exfoliation of solid materials with naturally layered structures<sup>[4]</sup> in analogy to the formation of graphene from bulk graphite, for example the semiconductor MoS<sub>2</sub>;<sup>[4a,5]</sup> 3) the unzipping of intrinsically layered single-walled or multiwalled carbon nanotubes by chemical and

physical means;<sup>[6]</sup> 4) the release from bulk semiconductor substrates not occurring in layers, for example, silicon, through the complex combination of anisotropic etching, metal deposition, and lithographic procedures;<sup>[7]</sup> 5) the epitaxial-based growth of releasable sacrificial multilayer assemblies for the formation of GaAs NRs;<sup>[8]</sup> and 6) the use of wafer-bonded layered materials, for example, silicon-on-insulator, followed by the release of NMs by selective etching of the buried oxide layer.<sup>[9]</sup> Unlike the richly developed, and almost unlimited, synthetic methods for NW structures, synthetic approaches for NRs suffer from several restrictions, such as the limited control over the dimensions, morphology, chemical composition, and monodispersity of the resulting materials. Additionally, the present requirement of specialized and complex etching procedures, the use of lithography for controlling the lateral dimensions of NRs, and strict epitaxy- and bonding-related constraints severely limit the spectrum of accessible NR materials and the control over their width, thickness, length, chemical composition, shape, crystallinity, and on-substrate assembly. Thus, the discovery of new approaches for the design and unlimited synthetic realization of complex NR materials, with predictable morphology, composition, and physical properties, on the atomic scale and upwards, is of significant importance.

Herein, we demonstrate the development of a universal approach for the controlled formation of semiconducting NRs, with nearly 100 % yield, based on the “unwrapping” of precursor core–shell NW heterostructures. On-substrate GeSi core–shell NW heterostructures were synthesized through conventional chemical vapor deposition (CVD) procedures, by the conformal epitaxial overcoating of crystalline germanium NW cores with a silicon shell.<sup>[10]</sup> The top surface of the heterostructures was carved in a smooth, controllable fashion by anisotropic reactive-ion etching, and the sides were protected by a thin layer of photoresist material. In this way, the originally closed Si shell structure was sliced open prior to selective chemical removal of the sacrificial Ge core, resulting in the formation of crystalline, fully opened and flat NR structures (Figure 1). The width of the resulting NRs can be readily controlled by both the diameter of the Au catalysts employed for the growth of the germanium sacrificial core, as well as simply by the etching time applied for the top-carving of the closed Si shell structure. This allows for the versatile control over the lateral dimensions of the resulting NRs (Figure 1 and Figure 2a–e; Figure S4 in the Supporting Information). Figure 2a–e shows representative SEM images of Si NRs of decreasing width obtained by this approach: GeSi NW heterostructures (50 nm core diameter and 10 nm shell thickness) were carved using various etching

[\*] A. Pevzner,<sup>[a]</sup> G. Davidi,<sup>[a]</sup> H. Peretz-Soroka, E. Havivi, Prof. F. Patolsky  
School of Chemistry  
The Raymond and Beverly Sackler Faculty of Exact Sciences  
Tel Aviv University, Tel Aviv 69978 (Israel)  
Dr. Z. Barkay  
Wolfson Applied Materials Research Center  
Tel Aviv University, Tel Aviv 69978 (Israel)  
Dr. R. Popovitz-Biro  
Electron Microscopy Unit, Weizmann Institute of Science  
Rehovot (Israel)  
Dr. A. Khatchtourints, Prof. F. Patolsky  
The Center for Nanoscience and Nanotechnology  
Tel Aviv University, Tel Aviv 69978 (Israel)  
E-mail: fernando@post.tau.ac.il

[†] These authors contributed equally to this work.

[\*\*] We thank the Legacy Foundation for financial support.

Supporting information for this article is available on the WWW under <http://dx.doi.org/10.1002/ange.201304857>.

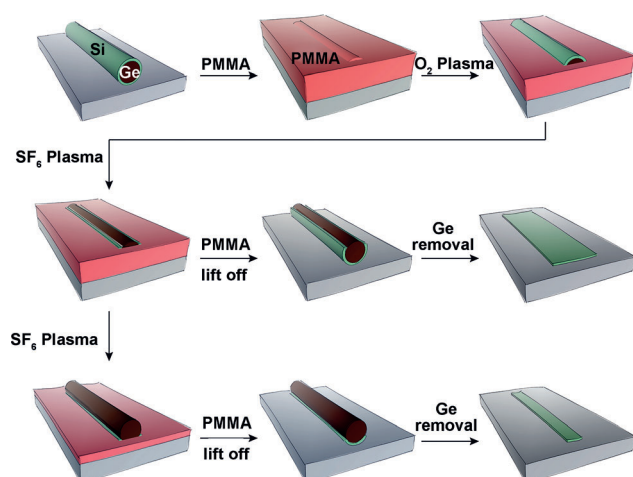


**Figure 1.** Schematic illustration of the unwrapping method for the formation of NRs. PMMA = polymethyl methacrylate.

times, and the Ge cores were removed by treatment with a mild  $\text{H}_2\text{O}_2$  solution.<sup>[10c]</sup> Notably, NRs of unprecedented ultrasmall widths ( $< 10$  nm) can be easily obtained by this simple approach. Clearly, germanium cores can be selectively removed by wet-chemical etching without affecting the integrity and the crystallinity of the epitaxially grown Si shells; the resulting Si NRs unfold and adhere to the support surface. The deposition of the precursor GeSi core-shell NWs on holey silicon nitride substrates allows for the formation and further TEM characterization of NR elements. HRTEM micrographs of typical Si NRs (Figure 2 f–h) demonstrate the uniformity and high-quality single-crystalline structure along their entire length. In addition, wide-field selected-area diffraction (SAED) (Figure 2g inset) further confirms that the resulting NRs are indeed single crystalline. The lattice-plane spacing (0.314 nm) obtained for a representative NR

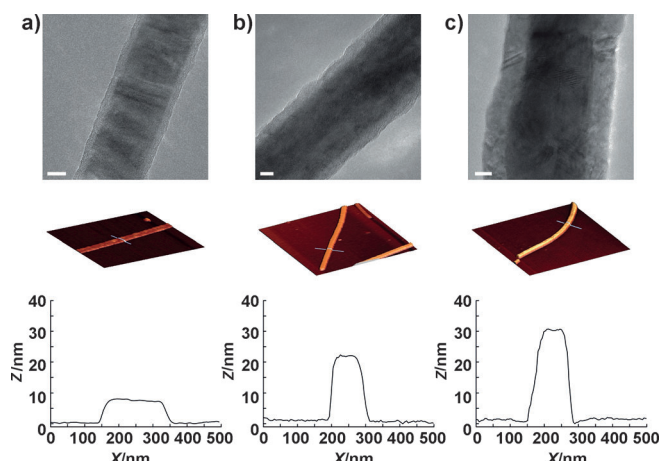


**Figure 3.** a–c) TEM images of the GeSi core-shell NWs of different shell thickness before unwrapping, and AFM images and profiles of the resulting Si NRs after the unwrapping process; scale bars 20 nm.

fits well with the interplanar distance of cubic silicon. The two-dimensional Fourier transform of the lattice-resolved image (Figure 2h inset) can be indexed to the diamond structure of silicon with a  $[111]$  growth direction. The resulting NRs are straight and smooth with a uniform width along their longitudinal axis. Moreover, it is also feasible to finely control the NR thickness (down to only 3 nm) by adjusting the deposition time of the silicon shell of the precursor NWs (Figure 3 a–c). Also, by altering the conditions for NW growth, it is possible to form NRs of varying predetermined tapered shapes (Figure S1 in the Supporting Information).

To shed light on the “unwrapping” mechanism resulting in NRs, the Ge cores of GeSi top-carved NW heterostructures were selectively removed by two methods (Figure 4): 1) treatment with  $\text{H}_2\text{O}_2$  solution (wet etching) and 2) treatment with  $\text{O}_2$  gas at  $500^\circ\text{C}$  (dry etching). It can be readily seen that the Si shell remaining after selective dry-etching of Ge cores resembles a “canoe-like” structure (Figure 4b), whereas the Si shell that remains after selective wet-etching of Ge cores completely unfolds and conformally adheres to the hosting substrate (Figure 4c). These results let us believe that capillary forces during the etching and drying steps play a significant role during the unwrapping process.

A unique advantage of our approach is the rational and precise control of the chemical composition of the NRs along their length and thickness axes, a task unattainable by existing synthetic methodologies. This can be ach-

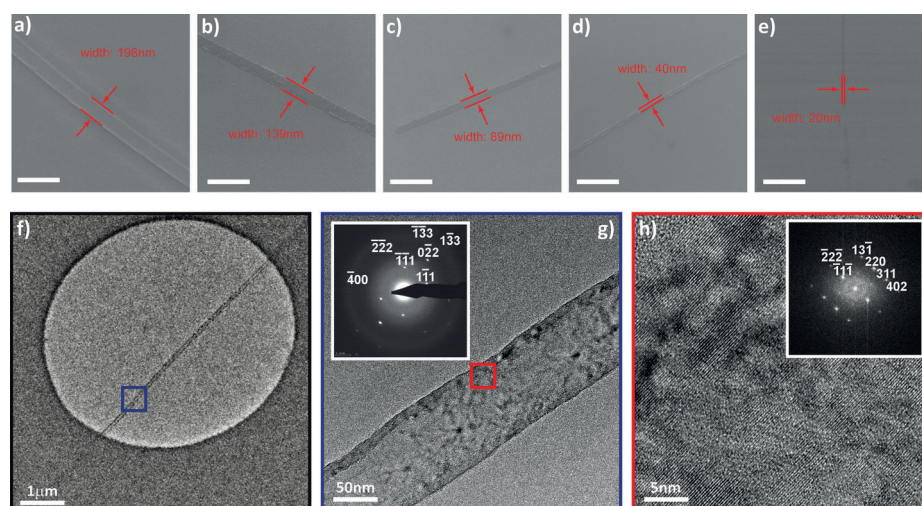


**Figure 2.** a–e) SEM images of the Si NRs with various widths obtained from GeSi nanowires (Si shell 10 nm, Ge core 50 nm) after different top-carving etching times; scale bars 500 nm. f, g) TEM images and the SAED (inset in (g)). h) HRTEM image of a Si NR and corresponding fast Fourier transform (FFT) image (inset).

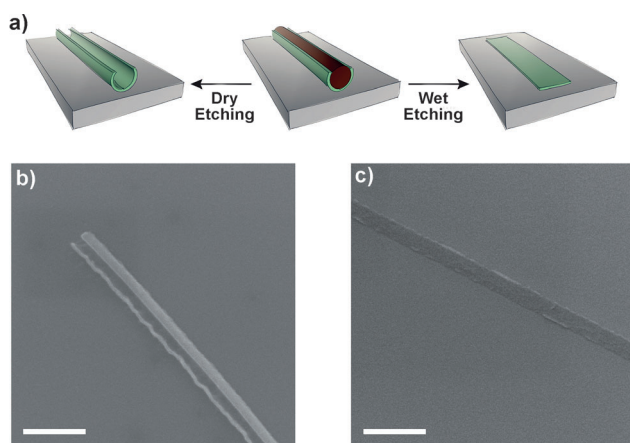


**Figure 4.** a) Schematic illustration of wet and dry etching of GeSi core-shell NWs. Si NRs obtained after removal of the Ge core by dry etching (b) and wet etching (c); scale bars 500 nm.

ieved by the direct doping of the shell structure during the synthesis of core-shell precursors, for single-shelled NWs, or by the formation of multielement alloy (or SiGe graded shell), such as Ge(core)-Si<sub>x</sub>Ge<sub>1-x</sub>(shell) NW precursors, before the formation of NRs. Figure 5a demonstrates the integration of p-type (1:4000 B/Si boron-doped) Si NR elements into electrical back-gated FET devices, and their evaluation by

electrical transport measurements. Figure 5a depicts the  $I_{ds}$  versus  $V_{ds}$  plot for an individual p-type Si NR FET at different gate voltages ( $V_g$ ), and the transconductance curve ( $I_{sd}$  vs.  $V_g$  at a constant  $V_{ds}=0.1$  V). The observed gate-voltage behavior is typical of p-type FETs<sup>[11]</sup> and similar to previously reported nanowire-based FET devices.<sup>[10a,12]</sup> In contrast, undoped intrinsic Si NRs and n-type (phosphorus-doped) Si NRs show electrical behaviors typical of that expected based on their composition. Furthermore, we have employed our doped NR elements as building blocks for the fabrication of FET sensing devices for the sensitive sensing of solution pH (Figure 5b).<sup>[12]</sup> The unmodified Si NW FETs (with pH-sensitive silanol surface groups) effectively and reversibly respond to changes over a wide pH range, pH 4–9, at physiological conditions at high ionic strength (10 mM phosphate buffer and 138 mM NaCl). This is caused by the protonation/deprotonation of pH-sensitive surface functional groups responsible for the pH-driven modulation of the FETs conductance, as previously reported.<sup>[12, 13]</sup>

A natural evolution from single-element structures has been towards the synthesis of complex multicomponent 1D NRs. The creation of heterojunctions has led to materials with multiple functionalities not realized with single-component nanostructures and useful in a broad range of applications.<sup>[14]</sup> In this regard, the ability to modulate a NR's chemical composition along its length, as well as its thickness, has not

yet been demonstrated by current methods. The chemical modulation of NRs along their thickness axis, can be directly achieved by the ab initio synthesis of Ge core-multishell NW precursors.<sup>[10b,c]</sup> The top-carving and subsequent unwrapping of NWs leads to the thickness-modulated doping of NRs, or thickness-modulated alloy-graded NRs. More importantly, and in order to solve the difficult challenge in modulating the chemical composition of NRs along their length axis, we developed the so-called “doping-reflection” approach (Figure 5c). By this method, we first synthesize axially modulated highly doped Ge core NWs composed of p- and n-type doped segments (P/Si and B/Si ratios of 1:500). Next, a shell of undoped intrinsic Si of controlled thickness is deposited. A high-temperature annealing step (750–850 °C) is then applied to promote the “radial” controlled diffusion of dopant atoms,<sup>[15]</sup> from the originally doped Ge core into the undoped Si shell. Figure 5d shows the current–voltage ( $I$ – $V$ ) plot recorded on a representative four-contact device fabricated from

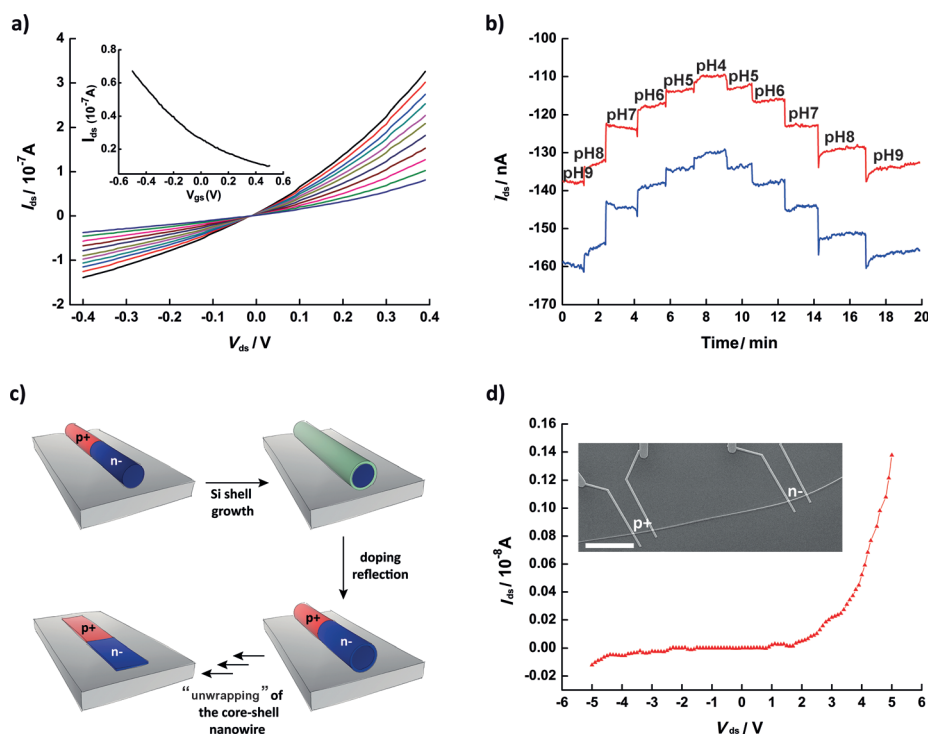


**Figure 5.** a) Plots of source-drain current ( $I_{ds}$ ) versus source-drain voltage ( $V_{ds}$ ) at different gate voltages ( $V_g$ ) ( $V_g$ =water gate) for a typical p-type Si NR FET: -0.5 V (black), -0.4 V (red), -0.3 V (blue), -0.2 V (green), -0.1 V (magenta), 0 V (dark yellow), 0.1 V (navy), 0.2 V (wine), 0.3 V (pink), 0.4 V (olive), and 0.5 V (royal blue); inset: Plot of  $I_{ds}$  versus  $V_g$  ( $V_g$ =water gate) (transconductance curve) recorded for the same p-type Si NR FET device at  $V_{ds}=0.1$  V. b) Changes in NR-FET conductance as the pH of solutions delivered to the sensor is varied from 9 to 4. c) Schematic illustration of the preparation of p-n Si NRs by the “doping reflection” procedure. d)  $I$ – $V$  plot for the p-n Si NR device; inset: SEM image of the p-n Si NR device; scale bar 5 μm.



a dual p/n-type-doped Si NR structure. A clear current rectification in reverse bias with an onset at a forward bias voltage is observed, consistent with the synthesis of a well-defined

p/n diode within the NR structure. These results show, for the first time, that dopant atoms in the sacrificial cores can be effectively “reflected” into the shell structures by simple time-controlled high-temperature annealing of the core-shell NW precursors, leading the formation of axially modulated NR heterostructures. Additionally, the formation of unprecedented crystallinity-modulated NRs along their length axis can be envisioned by applying our approach. Our approach may be further expanded for the creation of composite NR heterostructures, consisting of components other than semiconductor elements, such as dielectric, metallic, and organic materials and their combination. For instance, we have also demonstrated the formation of dielectric NRs (ZnO, alumina, titania, etc.) by the combination of CVD-ALD (ALD: atomic layer deposition) preparation of these materials shells on Ge NW precursors. Additionally, composite semiconductor-dielectric NRs, for example, Si/alumina or Si/ZnO, can be easily prepared with fine control over the physical and chemical attributes of the individual components. Furthermore, crystalline semiconducting NRs made of materials other than silicon can be readily envisioned from additional epitaxial core-shell NW precursors, given the possibility to selectively remove the sacrificial core material. For example, ZnO/GaN core-shell NWs<sup>[16]</sup> can be used for the formation of GaN NRs, after top etching of the GaN shell material and the selective removal of ZnO cores. Also, ZnS, SiGe alloy, GaP NRs may be prepared from the epitaxially grown Ge/ZnS, Ge/SiGe, ZnO/GaP core-shell precursors.<sup>[17]</sup>

The high-fidelity large-scale assembly of 1D nanomaterials, with controlled and uniform orientation and density at spatially well-defined locations on diverse substrates has been the focus of enormous research efforts for the last two decades.<sup>[18]</sup> While significant progress has been achieved for the assembly of NW materials, almost no reports have dealt with the large-scale controlled assembly of ultrathin and narrow NR building blocks due to the limited availability of synthetic methods. We have taken advantage of the recently well-developed methods for NW assembly<sup>[18a]</sup> in order to create large-scale arrays of NR elements. First, oriented contact-transfer of the precursor core-shell NWs is performed on the surface of interest. Then controlled top-carving and unwrapping of protected NWs provides the resulting NRs. Figure S5 shows the large-scale position-controlled assembly of NRs on different surfaces, from silicon wafers to flexible plastic substrates. Notably, this procedure can be applied on 3D carved surfaces of complex morphologies (Figure 6). Deposition of the core-shell NW precursors on sharply carved substrates mainly leads to the formation of suspended NW elements (Figure 6a). Suspended NWs slightly bend to some extent, depending on the nanowire's diameter, but never completely cover the sharply carved substrates. In situ unwrapping of the suspended NW precursors with shell thicknesses of less than 10 nm leads to the formation of NRs that adhere and perfectly conform to the 3D pre-existent curvature. This shows the extreme flexibility

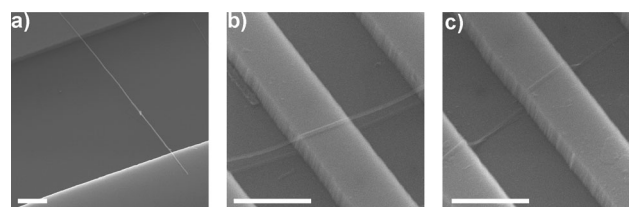


**Figure 6.** SEM images of a) a suspended Si NW with a thickness of 30 nm, b) a suspended Si NR with a thickness of approximately 30 nm, and c) a thinner Si NT with a thickness of less than 15 nm on 3D sharply carved substrates; scale bars 1  $\mu\text{m}$ .

of the resulting superthin and narrow NRs (Figure 6c). NR elements can conform to carved substrates even at the sharpest turning angles, without affecting their integrity and electrical conductivity. The conformal flexibility of NRs can be directly controlled by the thickness of the precursor NW's shells before its unwrapping. Thicker shells ( $> 15$  nm) tend to lead to partially, or totally, suspended NRs (Figure 6b). This mild and simple approach allows the direct on-surface formation of the thinnest and narrowest ever demonstrated NRs, without compromising the physical integrity of these intrinsically ultrasensitive materials. This is in contrast to current methods which involve the prior synthesis and subsequent transfer of NRs onto the device substrate.

To summarize, we have demonstrated a novel approach for the flexible, almost unlimited, synthesis of high-quality crystalline semiconducting NRs based on the on-substrate “unwrapping” of core-shell NW precursors. This versatile method allows for the unlimited fine-tuning of the following NR attributes: 1) NR thickness can be unprecedentedly controlled from ten of nanometers down to a few nanometers; 2) NR width can be readily controlled by the diameter of the parent NW heterostructure, as well as the time applied for carving the shell before the unwrapping occurs; this results in ribbons down to 10 nm in width or less; 3) The doping of single-element ribbons can be controlled during the NW shell deposition; 4) chemical composition of single-element and multiple-element alloyed ribbons is possible; 5) NR heterostructures with doping and chemical composition controlled along the cross section and length can be obtained by a newly developed “doping-reflection” approach; 6) The shape of the NRs can be controlled; 7) The formation of superthin NR elements (thickness  $< 10$  nm) on 3D-carved surfaces demonstrates their ability to intimately wrap around sharp indentations in the substrate. Also, the large-scale assembly<sup>[18a]</sup> of NR single elements on various substrates is demonstrated for the fabrication of surface-supported and suspended NRs-based FET electrical devices.

We believe that this powerful and simple nanotectonic approach, combining advantages from the bottom-up and top-down paradigms, will allow the future full exploitation of NR-based materials and their respective intriguing applications.

Received: June 6, 2013

Published online: September 13, 2013

**Keywords:** heterostructures · nanoribbons · nanostructures · semiconductors · silicon

- [1] a) C. M. Lieber, *Solid State Commun.* **1998**, *107*, 607–616; b) Y. Xia, P. Yang, Y. Sun, Y. Wu, B. Mayers, B. Gates, Y. Yin, F. Kim, H. Yan, *Adv. Mater.* **2003**, *15*, 353–389; c) Y. Weizmann, F. Patolsky, I. Popov, I. Willner, *Nano Lett.* **2004**, *4*, 787–792.
- [2] a) Y. Huang, C. M. Lieber, *Pure Appl. Chem.* **2004**, *76*, 2051–2068; b) R. Agarwal, C. M. Lieber, *Appl. Phys. A* **2006**, *85*, 209–215; c) F. Valentini, M. Carbone, G. Palleschi, *Anal. Bioanal. Chem.* **2013**, *405*, 451–465; d) A. S. Aricò, P. Bruce, B. Scrosati, J. M. Tarascon, W. Van Schalkwijk, *Nat. Mater.* **2005**, *4*, 366–377; e) M. Law, J. Goldberger, P. D. Yang, *Annu. Rev. Mater. Res.* **2004**, *34*, 83–122; f) R. Elnathan, M. Kwiat, A. Pevzner, Y. Engel, L. Burstein, A. Khatchourints, A. Lichtenstein, R. Kantaev, F. Patolsky, *Nano Lett.* **2012**, *12*, 5245–5254; g) Y. Engel, R. Elnathan, A. Pevzner, G. Davidi, E. Flaxer, F. Patolsky, *Angew. Chem.* **2010**, *122*, 6982–6987; *Angew. Chem. Int. Ed.* **2010**, *49*, 6830–6835.
- [3] a) K. R. Symon, *Mechanics*, 3rd ed., Addison-Wesley, Reading, MA, **1971**; b) J. A. Rogers, M. G. Lagally, R. G. Nuzzo, *Nature* **2011**, *477*, 45–53.
- [4] a) K. S. Novoselov, D. Jiang, F. Schedin, T. J. Booth, V. V. Khotkevich, S. V. Morozov, A. K. Geim, *Proc. Natl. Acad. Sci. USA* **2005**, *102*, 10451–10453; b) M. Osada, T. Sasaki, *J. Mater. Chem.* **2009**, *19*, 2503–2511; c) R. Ma, T. Sasaki, *Adv. Mater.* **2010**, *22*, 5082–5104.
- [5] a) G. D. Davis, P. E. Viljoen, M. G. Lagally, *J. Electron Spectrosc. Relat. Phenom.* **1980**, *20*, 305–318; b) B. Radisavljevic, A. Radenovic, J. Brivio, V. Giacometti, A. Kis, *Nat. Nanotechnol.* **2011**, *6*, 147–150.
- [6] a) D. V. Kosynkin, A. L. Higginbotham, A. Sinitskii, J. R. Lomeda, A. Dimiev, B. K. Price, J. M. Tour, *Nature* **2009**, *458*, 872–U875; b) L. Jiao, L. Zhang, X. Wang, G. Diankov, H. Dai, *Nature* **2009**, *458*, 877–880; c) M. Terrones, *ACS Nano* **2010**, *4*, 1775–1781.
- [7] H. C. Ko, A. J. Baca, J. A. Rogers, *Nano Lett.* **2006**, *6*, 2318–2324.
- [8] J. Yoon, S. Jo, I. S. Chun, I. Jung, H. S. Kim, M. Meitl, E. Menard, X. L. Li, J. J. Coleman, U. Paik, J. A. Rogers, *Nature* **2010**, *465*, 329–U380.
- [9] S. Kim, J. Wu, A. Carlson, S. H. Jin, A. Kovalsky, P. Glass, Z. Liu, N. Ahmed, S. L. Elgan, W. Chen, P. M. Ferreira, M. Sitti, Y. Huang, J. A. Rogers, *Proc. Natl. Acad. Sci. USA* **2010**, *107*, 17095–17100.
- [10] a) L. J. Lauhon, M. S. Gudixsen, C. L. Wang, C. M. Lieber, *Nature* **2002**, *420*, 57–61; b) M. Ben-Ishai, F. Patolsky, *Adv. Mater.* **2010**, *22*, 902–906; c) M. B. Ishai, F. Patolsky, *Angew. Chem.* **2009**, *121*, 8855–8858; *Angew. Chem. Int. Ed.* **2009**, *48*, 8699–8702.
- [11] F. Patolsky, G. F. Zheng, C. M. Lieber, *Nat. Protoc.* **2006**, *1*, 1711–1724.
- [12] Y. Cui, Q. Q. Wei, H. K. Park, C. M. Lieber, *Science* **2001**, *293*, 1289–1292.
- [13] H. Peretz-Soroka, A. Pevzner, G. Davidi, V. Naddaka, R. Tirosh, E. Flaxer, F. Patolsky, *Nano Lett.* **2013**, *13*, 3157–3168.
- [14] a) T. J. Kempa, B. Tian, D. R. Kim, J. Hu, X. Zheng, C. M. Lieber, *Nano Lett.* **2008**, *8*, 3456–3460; b) M. Ben-Ishai, F. Patolsky, *Nano Lett.* **2012**, *12*, 1121–1128.
- [15] F. L. Via, C. Spinella, E. Rimini, *Semicond. Sci. Technol.* **1995**, *10*, 1362.
- [16] J. Goldberger, R. R. He, Y. F. Zhang, S. W. Lee, H. Q. Yan, H. J. Choi, P. D. Yang, *Nature* **2003**, *422*, 599–602.
- [17] a) J. Hu, Y. Bando, Z. Liu, J. Zhan, D. Golberg, T. Sekiguchi, *Angew. Chem.* **2004**, *116*, 65–68; *Angew. Chem. Int. Ed.* **2004**, *43*, 63–66; b) G. Shen, Y. Bando, C. Ye, X. Yuan, T. Sekiguchi, D. Golberg, *Angew. Chem.* **2006**, *118*, 7730–7734; *Angew. Chem. Int. Ed.* **2006**, *45*, 7568–7572; c) X. M. Shuai, W. Z. Shen, *J. Phys. Chem. C* **2011**, *115*, 6415–6422.
- [18] a) Y.-Z. Long, M. Yu, B. Sun, C.-Z. Gu, Z. Fan, *Chem. Soc. Rev.* **2012**, *41*, 4560–4580; b) A. Pevzner, Y. Engel, R. Elnathan, T. Ducobni, M. Ben-Ishai, K. Reddy, N. Shpaisman, A. Tsukernik, M. Oksman, F. Patolsky, *Nano Lett.* **2010**, *10*, 1202–1208; c) A. Pevzner, Y. Engel, R. Elnathan, A. Tsukernik, Z. Barkay, F. Patolsky, *Nano Lett.* **2012**, *12*, 7–12.